Chemical Engineering Research Bulletin 14 (2010) 97-102 Available online at http://www.banglajol.info/index.php/CERB

# THE INFLUENCE OF NICKEL LOADING ON REDUCIBILITY OF NiO/$Al_2O_3$ CATALYSTS SYNTHESIZED BY SOL-GEL METHOD

**Mohammad Zangouei, Abdolsamad Zarringhalam Moghaddam*, Mehdi Arasteh**

***Department of Chemical Engineering, Tarbiat Modares University, P.O.Box: 14115-143, Tehran, Iran***

Received 18 May 2010; received in revised form 2 November 2010

**Abstract:** The sol-gel method was used to synthesize nickel-alumina catalysts with various nickel loadings. Chemical and physical properties of support and supported nickel were characterized by TGA, DTA, EDX, SEM, BET, XRD and TPR techniques. Calcination temperature (500°C) was determined by performing thermogravimetric analysis (TGA) and differential thermal analysis (DTA) on the samples. Energy dispersive X-ray (EDX) was used to determine the actual content of nickel on alumina. $N_2$ adsorption test revealed that the specific surface area varied between 550 and 223 $m^2/g$ for pure alumina and 30%Ni/Al, respectively. X-ray diffraction (XRD) patterns showed no peaks due to NiO species and NiO species were well dispersed on the support by formation of $NiAl_2O_4$ phase. Temperature-programmed reduction (TPR) indicated that the nickel species mainly presented in $NiAl_2O_4$ phase and small amount of NiO. In the 20 percent nickel loading, the surface $NiAl_2O_4$ phase, which is between NiO and bulk $NiAl_2O_4$ phases in terms reducibility, was formed considering as a successful result.

***Keywords:*** *Nickel-alumina catalysts, sol-gel method, thermogravimetric analysis, dispersion of NiO, reducibility*

***DOI:****10.3329/cerb.v14i2.5052*

## 1. Introduction

In recent years, catalytic reforming of hydrocarbons has been extensively used for hydrogen production. Greenhouse gases emitted from hydrocarbon fuels, cause atmospheric pollution and global warming. However, when pure hydrogen is burnt, water and heat are the only products. Thus, hydrogen as a clean fuel is the best replacement for fossil fuels [1–3].

For catalytic reforming of hydrocarbons, a catalyst with high surface area, thermal stability and resistance toward deactivation of active phases is required. This has been a main subject of many researches in recent years [4–7].

Many researchers have reported that the sol-gel method can be used for synthesis of supported metal catalysts with high, uniform and stable metal dispersion [8, 9]. For example, it has been reported that nickel-alumina synthesized by sol-gel method has more stable support structure and higher nickel dispersion than those catalysts synthesized by conventional methods such as impregnation [5]. In this method, physicochemical properties of catalysts like porosity and surface area are controllable by pretreatment steps such as aging, drying, calcination and other synthesis conditions. Different supported metals such as Co, Cu, Ni, Pt and Rh have been used to catalytic reforming of hydrocarbons [10–12].

It has been reported that Rh-supported catalysts have the highest activity and stability toward deactivation [13]. However, they are very expensive. Therefore, the cheaper metals like Co, Fe and Ni supported on various oxides such as $SiO_2$, $Al_2O_3$, ZnO, MgO and $ZrO_2$ have attracted the attention of many researchers. Among them, nickel-alumina catalysts have been extensively used because of low cost, good thermal stability, high specific surface area and relatively high catalytic activity [13–15]. However, in spite of many studies and attempts, no efficient nickel catalysts with desirable properties have been established yet.

In the nickel-alumina catalysts, NiO species can be presented in two forms: free NiO species on the surface of $Al_2O_3$ or incorporated with $Al_2O_3$ to form $NiAl_2O_4$. Free NiO species are easily reduced to Ni particles. However, they are sintered more than $NiAl_2O_4$ during the thermal treatment, resulting in catalyst deactivation. The extent incorporation of $Ni^{2+}$ with $Al_2O_3$ depends on the chemical properties of the support, preparation conditions and amount of nickel loading [16]. In other words, when the chemical properties of the support and preparation conditions are fixed, the extent incorporation of $Ni^{2+}$ with $Al_2O_3$ could be properly controlled by changes in nickel loading amount. On the other hand, most of researchers have synthesized bulk $NiAl_2O_4$ phase or free NiO species on $Al_2O_3$ as a catalyst, causing weak reducibility and high sintering of active sites, respectively. Indeed, reports on synthesis of surface $NiAl_2O_4$ phase as a catalyst have been rarely published.

In the present work, in order to synthesize surface $NiAl_2O_4$ phase, which is between NiO and bulk $NiAl_2O_4$ phases in terms of nickel-support interaction (reducibility), four samples of NiO/$Al_2O_3$ catalyst were synthesized with various nickel loadings (5, 10, 20 and 30%). All samples were synthesized by sol-gel method. The fundamental objective was to determine the optimum nickel loading for the minimization of reducibility temperature.

---

* Corresponding author, Email:zarrin@modares.ac.ir

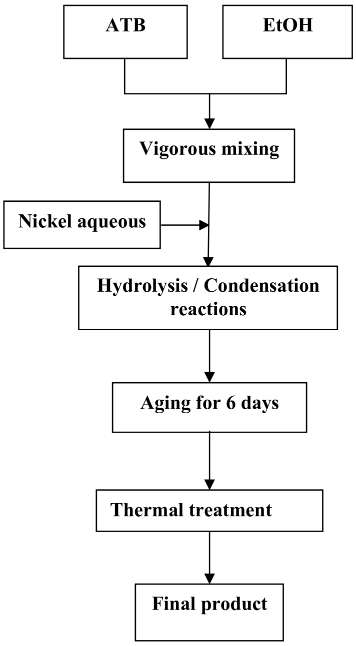

Figure 1: Schematic procedure for the preparation of nickel-alumina catalysts synthesized by sol-gel method

## 2. Experimental Procedure

### 2.1. Catalyst preparation

Nickel-alumina catalysts with different nickel contents were synthesized using sol-gel method. $Ni(NO_3)_2 \cdot 6\,H_2O$ with over 99% purity was used for the nickel precursor. Aluminum tri-sec-butoxide (ATB, $>$ 97%) was used as an aluminum precursor. All the above chemical agents were supplied by Merck Company. The preparation process began by gradual adding of ATB into ethanol while being stirred vigorously. Pre-dissolved nickel precursor in a required amount of deionized water was added into suspension of ATB and ethanol at a flow rate of 2 ml/min. During the adding of aqueous nickel precursor, a green gel was formed. The color of the gel changed from light green to dark green with the increase of nickel loading. For pH adjustment of the obtained gel, $NH_4OH$ or $HNO_3$ (65%) was slowly added into the resulting gel. The molar ratio of used precursors for preparation of catalysts is shown in Table 1. The gel was stirred for 1 h and then aged for 6 days at ambient temperature. The aged gel was dried in oven at 100°C for 12 h. For calcination, the samples were heated up to 500°C at 10°C/min and held for 4 h under static air atmosphere. Schematic procedure for preparation of nickel-alumina catalysts using sol-gel method is presented in Figure 1. The synthesized nickel-alumina catalysts were assigned as XNi/Al, where X is the percentage weight of nickel in the catalyst.

### 2.2. Catalyst characterization

The crystalline phases of support and supported nickel catalysts were identified by XRD with Cu kα radiation (Philips Xpert, $\gamma = 0.15406$ nm) at 40 kV and 40 mA. The measurements were carried out in steps of 0.02°/sec in the 2θ range of 10-80°.

Table 1: Molar ration of the precursors and acidity of the resulting gel

| Catalyst | Molar ration and acidity | | | |
|---|---|---|---|---|
| | ATB | $H_2O$ | EtOH | pH |
| Pure $Al_2O_3$ | 1 | 3.6 | 26.4 | 5.2 |
| 5 Ni/Al | 1 | 3.6 | 26.4 | 5.1 |
| 10 Ni/Al | 1 | 3.6 | 26.4 | 5.0 |
| 20 Ni/Al | 1 | 3.6 | 26.4 | 5.0 |
| 30 Ni/Al | 1 | 3.6 | 26.4 | 5.0 |

Thermal stability and structure destruction of the support and supported nickel catalysts were investigated by TGA and DTA at a heating rate of 10°C/min up to 700°C. The weight of samples was 8 mg under sweeping air atmosphere at 10 ml/min (PL Thermal Science STA 1500).

Scanning electron microscopy (SEM) images were taken on a Philips XL 30 operating at an accelerating voltage from 5 to 30 kv. The samples were coated with a thin film of gold on their surface using a sputtering device. In order to determine the actual and uniform nickel loading, EDX analysis was used.

The specific surface area and pore volume of the samples were determined by $N_2$ adsorption at 77 k (Micromeritics Gemini 2375 V4.02) previously degassed at 150°C for 2 h.

TPR was performed on Quantachrome CHEMBET 3000 apparatus to investigate the reducibility of the samples. Before analysis, by passing argon over the samples, they were degassed at 100°C for 1 h. After pretreatment, the samples were heated up to 950°C at a heating rate of 10°C/min. The heated samples were held at 950°C for 10 min. The flow was 7% $H_2$/Ar (10 ml/min).

## 3. Results and Discussion

### 3.1. Physiochemical properties of synthesized catalysts

The pH of the resulting gel, EtOH/ATB and $H_2O$/ATB molar ratio were fixed in order to investigate the effect of nickel loading on the specific surface area and pore volume of samples. Table 2 shows the effect of nickel loading on the specific surface area and pore volume of nickel-alumina catalysts. The results show that the specific surface area and pore volume of the catalysts decreased with the increase of nickel loading, probably due to blockage of the support pores by NiO particles. Pure support ($\gamma$-$Al_2O_3$) and 30Ni/Al catalysts showed the highest (550 $m^2$/g) and the lowest (223 $m^2$/g) specific surface area, respectively.

### 3.2. Morphology of support and supported nickel catalysts

The surface morphology of nickel-alumina and $\gamma$-$Al_2O_3$ catalysts were studied by SEM (Fig. 2). As illustrated in

Table 2: Physical properties of the catalysts calcined at 500°C for 4 h

| Catalysis | Amount of Ni used (%wt) | Actual Ni content (%wt) | Specific surface area ($m^2$/g) | Pore volume ($cm^3$/g) |
|---|---|---|---|---|
| Pure $Al_2O_3$ | - | - | 550 | 0.923 |
| 5 Ni/Al | 4.9 | 5 | 505 | 0.427 |
| 10Ni/Al | 9.6 | 10 | 423 | 0.442 |
| 20Ni/Al | 19.1 | 20 | 314 | 0.307 |
| 30Ni/Al | 29.4 | 31 | 223 | 0.245 |

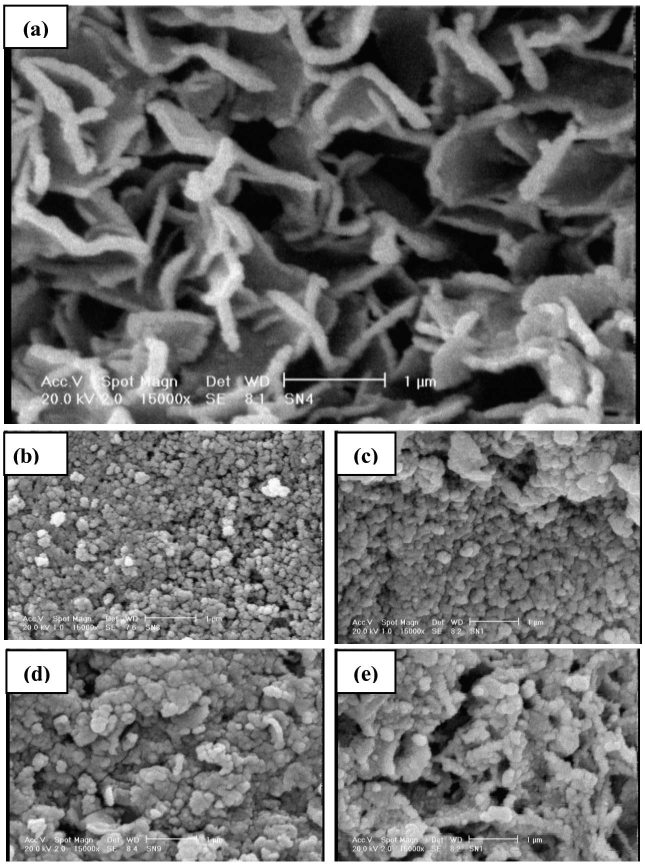

Figure 2: SEM images of (a) Pure γ-$Al_2O_3$, (b) 5Ni/Al, (c) 10Ni/Al, (d) 20 Ni/Al and (e) 30Ni/Al catalysts calcined at 500°C for 4 h (scale: 1 $\mu$m)

Fig. 2a, the γ-$Al_2O_3$ catalyst has a very high porous structure, which is in good agreement with this sample's high surface area. Other images present the surface morphology of nickel-alumina catalysts with various nickel loadings.

### 3.3. *Thermal analysis of synthesized catalysts*

TGA and DTA were carried out to study the weight loss, thermal behavior and structural destruction of the samples in the calcination treatment.

Figure 3 shows the results of TGA and DTA analysis for non-calcined support. The observed TGA curve showed 37% as total weight loss that occurred at two temperature regions. The first region occurred from room temperature to 130°C and reached a maximum at 73°C, which corresponded to the removal of the whole organic solvent, bulk water and physisorbed water. The first endothermic peak in the DTA curve related to this process. Weight loss at the second temperature region began from 180°C and ended at 569°C. In this region, two endothermic peaks were observed, which occurred at 225°C and 415°C, respectively. They were attributed to the removal of structure water from the support that can be presented by the following equations [17, 18]:

$$\mathrm{AlO(OH)\cdot nH_2O} \longrightarrow \mathrm{AlO(OH)} + \mathrm{nH_2O} \tag{1}$$

$$2\,\mathrm{AlO(OH)} \longrightarrow \gamma\mathrm{-Al_2O_3} + \mathrm{H_2O} \tag{2}$$

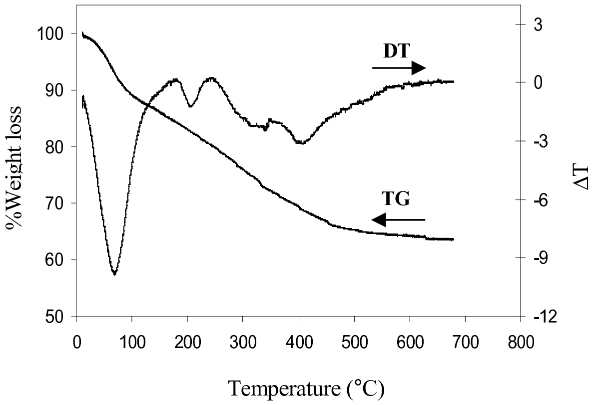

Figure 3: TGA and DTA analysis for non-calcined support

The percentage weight loss in the first and second regions was found to be 13 and 24%, respectively. For the typical non-calcined supported nickel catalyst (Figure 4), the total weight loss was 47%. This weight loss occurred at two temperature regions. The first region occurred between 25 and 168°C and reached to a maximum at 80°C. The weight loss in this region was obtained as 13%. It should be related to removal of residual ethanol (organic solvent), bulk water and physisorbed water. In DTA profile, the first endothermic peak at 80°C is related to the first weight loss region. The second weight loss region happened at the temperature range of 170-420°C, where a broad endothermic peak between 170 and 350°C with maximum at 300°C in DTA curve was observed relating to the decomposition of nickel nitrate entrapped in the pores of the support [5]. The amount of weight loss at the second region was found to be 31% of the sample weight. The total weight loss of the supported nickel sample was more than the total weight loss of the support, as expected. This difference is related to the dissociation of nickel nitrate presented in the supported nickel sample. As it can be seen, there were no appreciable thermal changes and weight loss when the sample was heated above 500°C and it was considered as calcination temperature.

The results of TGA and DTA analysis of the calcined supported nickel sample are presented in Figure 5. The total weight loss was about 3.5 % that occurred in one step from room temperature to 188°C with an endothermic peak at 80°C. It can be attributed to the removal of water adsorbed on the sample. There were no thermal and weight changes with further increase of temperature. Therefore, it can be confirmed that calcination treatment at 500°C for 4 h caused the removal of the whole solvent, bulk and structure water from the samples as well as complete decomposition of nickel nitrate into nickel oxide.

### 3.4. *Crystalline structure and phase of catalysts*

The XRD analysis was performed to study the crystalline structure of the samples. Figure 6 shows the XRD patterns of sol-gel synthesized γ-$Al_2O_3$ (calcined at 500°C for 4 h) and commercial γ-$Al_2O_3$. The spectrum of the commercial

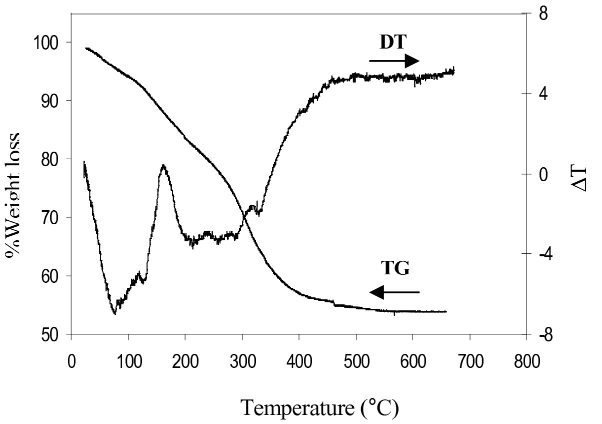

Figure 4: TGA and DTA analysis for typical noncalcinedsupported nickel

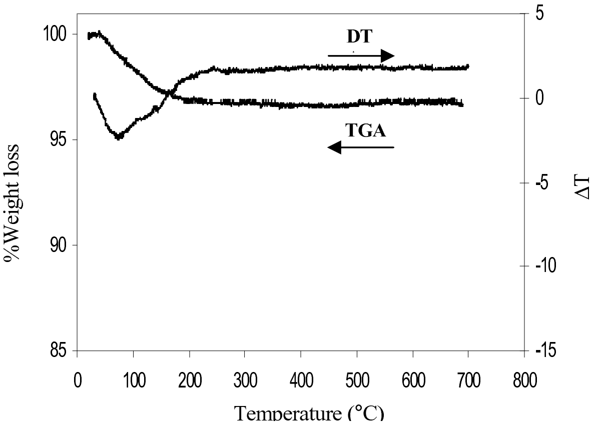

Figure 5: TGA and DTA analysis for typical calcined supported nickel

$\gamma$-$Al_2O_3$ is shown for comparison. The XRD spectrum of the synthesized $\gamma$-$Al_2O_3$ showed very low and broad peaks indicating that the sample was in amorphous form. This is confirmed by high specific surface area of this sample. On the other hand, XRD spectrum of the commercial $\gamma$-$Al_2O_3$ showed relatively sharp and intense peaks indicating high crystallinity and presence of bigger crystallite size comparing to the synthesized $\gamma$-$Al_2O_3$ sample. The crystallite size of both samples was calculated through Scherrer equation. The crystallite size of the commercial $\gamma$-$Al_2O_3$ was found about 6.8 nm, while that of the synthesized $\gamma$-$Al_2O_3$ could not be calculated because its size was smaller than the detection limit of XRD measurements. It is noteworthy that XRD can only calculate crystalline sizes that are larger than 2-5 nm [16].

The XRD patterns of the supported nickel samples with various nickel loadings are presented in Figure 7. All samples were calcined at 500°C for 4 h. The XRD patterns revealed that the support and supported nickel samples had low crystallinity phase as evidenced by the broad peaks assigned to the presence of $\gamma$-$Al_2O_3$ and $NiAl_2O_4$ phases, respectively. This low crystallinity is in very good agreement with the high

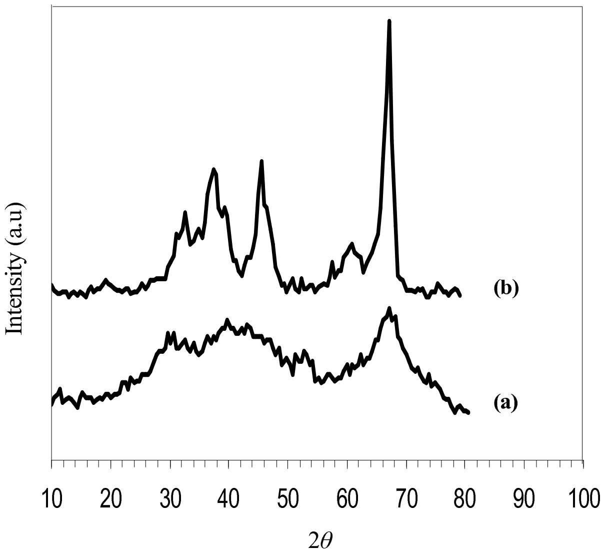

Figure 6: XRD patterns of (a) sol-gel synthesized $\gamma$-$Al_2O_3$ calcined at 500°C for 4 h, and (b) commercial $\gamma$-$Al_2O_3$

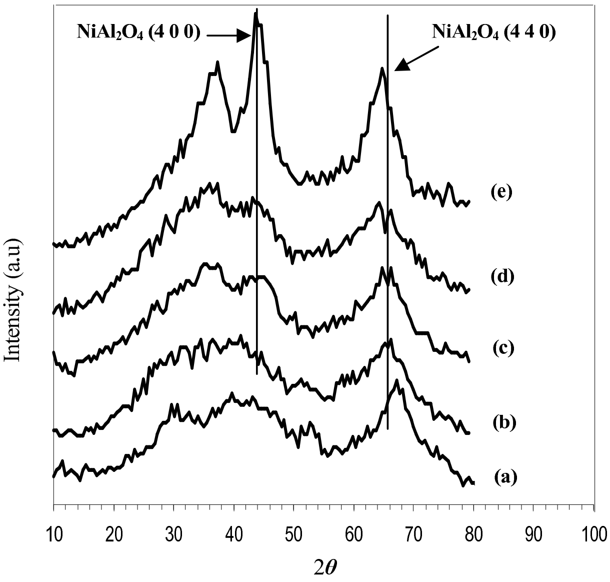

Figure 7: XRD patterns of (a) sol-gel synthesized $\gamma$-$Al_2O_3$, (b) 5Ni/Al, (c) 10Ni/Al, (d) 20Ni/Al and (e) 30Ni/Al calcined at 500°C for 4 h

specific surface area of these samples. When the nickel was loaded on the support, the main diffraction peak of $\gamma$-$Al_2O_3$ shifted to lower angles; this was due to diffusion of NiO particles into the support structure to form the $NiAl_2O_4$phase. No diffraction peaks, attributed to the nickel oxide, were observed even at 30% nickel loading. This result indicates that nickel particles are highly dispersed even at high nickel loadings by formation of $NiAl_2O_4$ phase and possibly very fine NiO species. The position of (4 4 0) diffraction peak, relating to $NiAl_2O_4$, slightly shifted to lower angles with the increase of nickel loading. This is due to the formation of de-

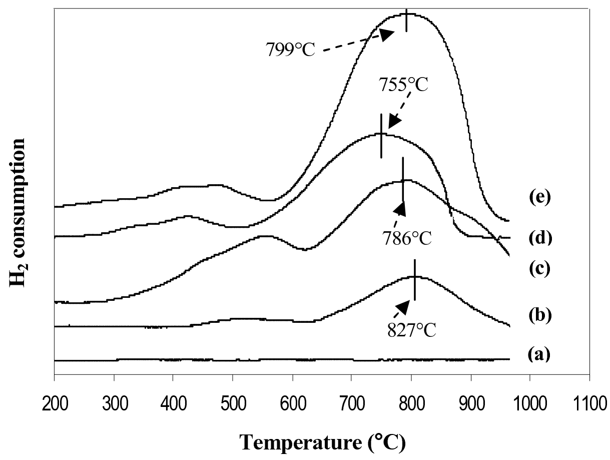

Figure 8: TPR curves for (a) sol-gel synthesized γ-$Al_2O_3$, (b)5 Ni/Al, (c) 10Ni/Al, (d) 20Ni/Al and (e) 30Ni/Al catalysts

fect spinel $NiAl_2O_4$ phase [13]. Further, it has been reported that the shift of the main diffraction peak is dependent on the amount of NiO species in the $Al_2O_3$ support [19].

### *3.5. Metal-support interaction*

To study the reducibility of NiO species and metal-support interaction, TPR experiments were performed. TPR test was also performed on the support (γ-$Al_2O_3$) for comparison purpose. The results showed that the support had no $H_2$ consumption peak indicating that it retained the oxide form as expected (Figure 8). For all the supported nickel samples, the TPR curves showed two sets of $H_2$ consumption peaks. The first set of peaks occurred at temperatures lower than 610°C (low temperature reduction peak). These peaks were attributed to the reduction of bulk NiO species with different extent interactions with the support. The second set appeared around 800°C (high temperature reduction peak) corresponding to the reduction of $NiAl_2O_4$ phases [20, 21]. The XRD patterns of these samples showed no diffraction peaks corresponding to the presence of NiO species. This is possibly due to the excellent dispersion of NiO species on the support and the crystallite sizes were smaller than detection limit of XRD measurements [22].

It is emphasized in the literature that the reducibility of nickel-alumina catalysts strongly depends on the interaction between NiO species and the support. For 5Ni/Al catalyst, the reduction of bulk $NiAl_2O_4$ phase occurred at 827°C represented by a single peak. As the nickel loading increased to 10%, the high temperature reduction peak shifted to 786°C, indicating the decrease of metal-support interaction. For these two samples, the low temperature reduction peak was observed at the temperature range of 450-610°C relating to the relatively strong NiO interaction with the support. With increasing of nickel loading to 20%, the high and low temperature reduction peaks shifted to 755 and 430°C, respectively. These peaks are related to the reduction of surface $NiAl_2O_4$ phase and weak interacted NiO-support species, respectively [21]. It is well known that the surface $NiAl_2O_4$ phase is more reducible than the bulk $NiAl_2O_4$ phase and also has more resistance to sintering, compared to free NiO species. It has been reported that interaction between nickel species and alumina decreases with the increase of nickel loading. However, in this work, a reversed pattern of temperature change was observed by passing from 20Ni/Al to 30Ni/Al catalyst, increasing from 755°C (20Ni/Al) to 799°C (30Ni/Al), which indicates an increase in metal-support interaction. It is believed that in the 20Ni/Al catalyst, most of nickel species were located on the surface of alumina, while in the 30Ni/Al catalyst most of them were located in the bulk of alumina. Indeed, the surface $NiAl_2O_4$ phase, which is between NiO and bulk $NiAl_2O_4$ phases in terms of reducibility (metal-support interaction), was formed in the 20Ni/Al catalyst using sol-gel method.

## 4. Conclusion

Sol-gel method was used to synthesize nickel-alumina catalysts with various nickel loadings. The effect of nickel loading on the specific surface area and pore volume was studied. It was found that both specific surface area and pore volume decreased with the increase of nickel loading. The TGA/DTA analysis of the calcined and non-calcined catalysts revealed that calcination at 500°C for 4 h caused the removal of the whole organic solvent, bulk and structural water. It also led to the complete decomposition of nickel nitrate into nickel oxide. The XRD patterns of calcined catalysts showed that nickel species well dispersed on γ-$Al_2O_3$ by formation of $NiAl_2O_4$ phase. The TPR results showed that reducibility of catalysts increased in the sequence of 5Ni/Al (827°C) $<$ 30Ni/Al (799°C) $<$ 10Ni/Al (786°C) $<$ 20Ni/Al (755°C). Therefore, the optimum nickel loading to obtain the maximum reducibility of nickel-alumina catalysts (formation of surface $NiAl_2O_4$ phase) and also stable towards sintering was found in 20% and this catalyst is promising to catalytic reforming of hydrocarbons.

## Acknowledgements

The authors are grateful to the National Iranian Oil Products Distribution Company (NIOPDC) for financial support. The authors also thank particularly Masood Vesali from Tehran University for the BET measurements.

## References

[1] Pakizeh M, Omidkhah M and Zarringhalam A, *Synthesis and characterization of new silica membranes using template-sol-gel technology*, International Journal of Hydrogen Energy, 2007. **32**(12):pp. 1825–1836. `doi:10.1016/j.ijhydene.2006.07.025`

[2] Cheekatamarla PK and Finnerty C, *Reforming catalysts for hydrogen generation in fuel cell applications*, Journal of Power Sources, 2006. **160**(1):pp. 490 – 499. `doi:10.1016/j.jpowsour.2006.04.078`

[3] Natesakhawat S, Watson RB, Wang X and Ozkan US, *Deactivation characteristics of lanthanide-promoted sol-gel* $Ni/Al_2O_3$ *catalysts in propane steam reforming*, Journal of Catalysis, 2005. **234**(2):pp. 496 – 508. `doi:10.1016/j.jcat.2005.07.014`

[4] Gonçalves G, Lenzi M, Santos O and Jorge L, *Preparation and characterization of nickel based catalysts on silica, alumina and titania obtained by sol-gel method*, Journal of Non-Crystalline Solids, 2006. **352**(32-35):pp. 3697 – 3704. doi:10.1016/j.jnoncrysol.2006.02.120

[5] Savva P, Goundani K, Vakros J, Bourikas K, Fountzoula C, Vattis D, Lycourghiotis A and Kordulis C, *Benzene hydrogenation over Ni/$Al_2O_3$ catalysts prepared by conventional and sol-gel techniques*, Applied Catalysis B: Environmental, 2008. **79**(3):pp. 199 – 207. doi:10.1016/j.apcatb.2007.10.023

[6] Hu L, Boateng KA and Hill JM, *Sol-gel synthesis of Pt/$Al_2O_3$ catalysts: Effect of Pt precursor and calcination procedure on Pt dispersion*, Journal of Molecular Catalysis A: Chemical, 2006. **259**(1-2):pp. 51 – 60. doi:10.1016/j.molcata.2006.06.018

[7] Kirumakki SR, Shpeizer BG, Sagar GV, Chary KV and Clearfield A, *Hydrogenation of Naphthalene over NiO/$SiO_2$-$Al_2O_3$ catalysts: Structure-activity correlation*, Journal of Catalysis, 2006. **242**(2):pp. 319 – 331. doi:10.1016/j.jcat.2006.06.014

[8] Kim J, DONG J, Park T and Kim K, *Effect of metal particle size on coking during $CO_2$ reforming of $CH_4$ over Ni-alumina aerogel catalysts*, Applied Catalysis A, General, 2000. **197**(2):pp. 191–200. doi:10.1016/S0926-860X(99)00487-1

[9] Zhang Y, Xiong G, Sheng S and Yang W, *Deactivation studies over NiO/[gamma]-Al2O3 catalysts for partial oxidation of methane to syngas*, Catalysis Today, 2000. **63**(2-4):pp. 517 – 522. doi:10.1016/S0920-5861(00)00498-3

[10] Shetty K, Zhao S, Cao W, Siriwardane U, Seetala N and Kuila D, *Synthesis and characterization of non-noble nanocatalysts for hydrogen production in microreactors*, Journal of Power Sources, 2007. **163**(2):pp. 630–636. doi:10.1016/j.jpowsour.2006.04.130

[11] Sanchez-Sanchez M, Navarro R and Fierro J, *Ethanol steam reforming over Ni/La-Al2O3 catalysts: Influence of lanthanum loading*, Catalysis Today, 2007. **129**(3-4):pp. 336–345. doi:10.1016/j.cattod.2006.10.013

[12] Vizcaíno A, Arena P, Baronetti G, Carrero A, Calles J, Laborde M and Amadeo N, *Ethanol steam reforming on Ni/Al2O3 catalysts: Effect of Mg addition*, International Journal of Hydrogen Energy, 2008. **33**(13):pp. 3489–3492. doi:10.1016/j.ijhydene.2007.12.012

[13] Kim P, Kim Y, Kim H, Song I and Yi J, *Synthesis and characterization of mesoporous alumina with nickel incorporated for use in the partial oxidation of methane into synthesis gas*, Applied Catalysis A: General, 2004. **272**(1-2):pp. 157–166. doi:10.1016/j.apcata.2004.05.055

[14] Tang S, Ji L, Lin J, Zeng HC, Tan KL and Li K, *CO2 Reforming of Methane to Synthesis Gas over Sol-Gel-made Ni/γ-$Al_2O_3$ Catalysts from Organometallic Precursors*, Journal of Catalysis, 2000. **194**(2):pp. 424 – 430. doi:10.1006/jcat.2000.2957

[15] Vos B, Poels E and Bliek A, *Impact of Calcination Conditions on the Structure of Alumina-Supported Nickel Particles*, Journal of Catalysis, 2001. **198**(1):pp. 77 – 88. doi:10.1006/jcat.2000.3082

[16] Li G, Hu L and Hill J, *Comparison of reducibility and stability of alumina-supported Ni catalysts prepared by impregnation and coprecipitation*, Applied Catalysis A: General, 2006. **301**(1):pp. 16–24. doi:10.1016/j.apcata.2005.11.013

[17] Nguefack M, Popa A, Rossignol S and Kappenstein C, *Preparation of alumina through a sol–gel process. Synthesis, characterization, thermal evolution and model of intermediate boehmite*, Physical Chemistry Chemical Physics, 2003. **5**(19):pp. 4279–4289. doi:10.1039/B306170A

[18] Kim S, Lee Y, Jun K, Park J and Potdar H, *Synthesis of thermostable high surface area alumina powder from sol-gel derived boehmite*, Materials Chemistry and Physics, 2007. **104**(1):pp. 56–61. doi:10.1016/j.matchemphys.2007.02.044

[19] Hao Z, Zhu Q, Jiang Z, Hou B and Li H, *Characterization of aerogel Ni/Al2O3 catalysts and investigation on their stability for CH4-CO2 reforming in a fluidized bed*, Fuel Processing Technology, 2009. **90**(1):pp. 113–121. doi:10.1016/j.fuproc.2008.08.004

[20] Kim P, Joo J, Kim H, Kim W, Kim Y, Song I and Yi J, *Preparation of Mesoporous Ni-alumina Catalyst by One-step Sol-gel Method: Control of Textural Properties and Catalytic Application to the Hydrodechlorination of o-dichlorobenzene*, Catalysis Letters, 2005. **104**(3):pp. 181–189. doi:10.1007/s10562-005-7949-5

[21] Alberton A, Souza M and Schmal M, *Carbon formation and its influence on ethanol steam reforming over Ni/$Al_2O_3$ catalysts*, Catalysis Today, 2007. **123**(1-4):pp. 257–264. doi:10.1016/j.cattod.2007.01.062

[22] JIANG H *et al.*, *Tri-reforming of methane to syngas over Ni/Al2O3–Thermal distribution in the catalyst bed*, Journal of Fuel Chemistry and Technology, 2007. **35**(1):pp. 72–78. doi:10.1016/S1872-5813(07)60012-7